*Imaging and Radiation Research (2023) Volume 6 Issue 2*
doi: 10.24294/irr.v6i2.6398

ORIGINAL RESEARCH ARTICLE

# Molecular dynamics simulation of atomic interaction between mediator protein of human prostate cancer and $Fe/C_{720}$ buckyballs-statin structures

**Mohammad Pour Panah[1], Roozbeh Sabetvand[2,*]**

[1] *Department of Physics, Faculty of Basic Sciences, Tarbiat Modares University, Tehran 14115-111, Iran*

[2] *Department of Energy Engineering and Physics, Faculty of Condensed Matter Physics, Amirkabir University of Technology, Tehran 159163-4311, Iran*

*** Corresponding author:** Roozbeh Sabetvand, r.sabetvand@gmail.com

## ABSTRACT

Atomic interaction between mediator protein of human prostate cancer (PHPC) and $Fe/C_{720}$ Buckyballs-Statin is important for medical science. For the first time, we use molecular dynamics (MD) approach based on Newton's formalism to describe the destruction of PHPC via $Fe/C_{720}$ Buckyballs-Statin with atomic accuracy. In this work, the atomic interaction of PHPC and $Fe/C_{720}$ Buckyballs-Statin introduced via equilibrium molecular dynamics approach. In this method, each PHPC and $Fe/C_{720}$ Buckyballs-Statin is defined by C, H, Cl, N, O, P, S, and Fe elements and contrived by universal force field (UFF) and DREIDING force-field to introduce their time evolution. The results of our studies regarding the dynamical behavior of these atom-base compounds have been reported by calculating the Potential energy, center of mass (COM) position, diffusion ratio and volume of defined systems. The estimated values for these quantities show the attraction force between Buckyball-based structure and protein sample, which COM distance of these samples changes from 10.27 Å to 2.96 Å after 10 ns. Physically, these interactions causing the destruction of the PHPC. Numerically, the volume of this biostructure enlarged from 665,276 $Å^3$ to 737,143 $Å^3$ by MD time passing. This finding reported for the first time which can be considered by the pharmaceutical industry. Simulations indicated the volume of the PHPC increases by $Fe/C_{720}$ Buckyballs-Statin diffusion into this compound. By enlarging this quantity (diffusion coefficient), the atomic stability of PHPC decreases and protein destruction procedure fulfilled.

***Keywords:*** human prostate; atomic buckyball; molecular dynamic method; atomic interaction; diffusion ratio

**ARTICLE INFO**

Received: 14 May 2024
Accepted: 13 June 2024
Available online: 18 July 2024



## 1. Introduction

The prostate is a gland in the male reproductive system that stabilized in vicinity of urethra just below the bladder from biological view[1]. Most prostate cancers are slow growing in this region of human body[2,3]. But, prostate cancer cells can be spread to other regions of human body[4]. It may initially cause no symptoms[5]. In the next evolution steps of this type of cancer, symptoms include pain or difficulty urinating, blood in the urine, or pain in the pelvis or back[1]. Benign prostatic hyperplasia may produce similar symptoms[1]. Other late symptoms include fatigue, due to low levels of red blood cells[1]. Clinically, important parameters which increased the risk of this cancer include older age, race, and family history[6,7]. Other biological parameters such as a diet high in processed meat (or red meat), while the risk from a high intake of milk products is inconclusive[8]. An association with gonorrhea detected, although no scientific description for this cancer

performance reported[9]. An increased risk is associated with the BRCA mutations[10]. Diagnosis is by biopsy. Medical imaging may be done to assess whether metastasis is present[11].

In actual cases, physicians have established cancer cell lines to predict the disease progress. Various techniques used for this purpose such as LNCaP, PC3, and DU145. The LNCaP cancer cell line was established from a human lymph node metastatic lesion of prostatic adenocarcinoma. PC3 and DU145 cells were established from human prostatic adenocarcinoma metastatic to bone and to brain, respectively. LNCaP cells express AR, but PC3 and DU145 cells express very little or no AR. The proliferation of LNCaP cells is androgen-dependent but the proliferation of PC3 and DU145 cells is androgen-insensitive. Elevation of AR expression is often observed in advanced prostate tumors in patients[12–15]. Today, more than common methods in prostate cancer detection, new atomistic methods such as computer simulations can be used for clinical purposes. Technically, atomistic study of cancer protein evolution can provide effective cancer treatment methods.

According to our descriptions, atomic analysis of prostate cancer's mediator protein should be introduced new methods to treat patients. The chemical/atomic representation of mediator Protein of Human Prostate Cancer (PHPC) depicted in **Figure 1**[16]. Today, computer simulations used in numerous fields of science[17–20]. The representation of the evolution of one system by the performance of the other sample modeled after it is known as computer simulation. A model of an actual phenomenon in the form of a computer algorithm is used by a simulation. This mathematical description is made up of equations that duplicate the functional relationships within the actual phenomenon. Molecular dynamics (MD) approach is the exact type of computer simulation that is capable of describing the time dependent behavior of atom-base systems[21–23]. Today, this computational approach is widely used in living structures simulations[24,25]. In current research, theoretical calculations were performed to predict the atomic interaction between mediator protein in PHPC and Fe/$C_{720}$ Buckyballs-Statin system. A nanostructure is a structure of intermediate size between microscopic and molecular structures. Structurally, spherical nanoparticles have three dimensions on the nano-scale, i.e., the particle is between 0.1 and 100 nm in each spatial dimension. Buckyballs belong to this group. Here, we introduce this type of nanoparticles as a drug delivery-based structure to implementing destruction procedure to PHPC for the first time.

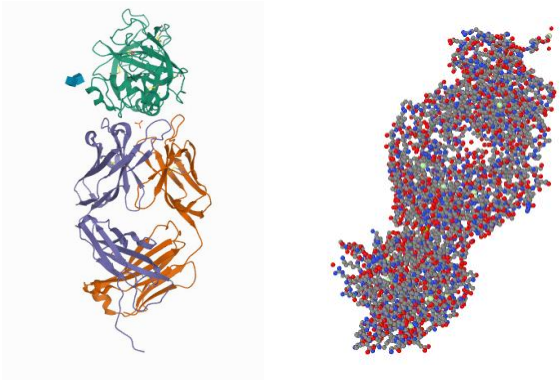

**(a)** **(b)**

**Figure 1.** Schematic of **(a)** chemical; **(b)** atomic arrangement of PHPC[16].

## 2. Computational method details

In this computational work, MD method in equilibrium condition has been used to estimate the atomic interaction between PHPC and Fe/$C_{720}$ Buckyballs-Statin structure at 300 K and $P$ = 1 bar[26]. In this method, atomic interaction is allowed for each time steps, providing an understanding of the atom-based systems evolution with time passing. Generally, solving Newton's equations of atom-base systems via computational algorithms, the trajectories of each atom are predicted where the interactions between them are computed by

force-field concept[27]. LAMMPS package has been used for the present MD simulations[28–31]. LAMMPS introduced us with different force-fields for MD description of soft structures such as protein-based compounds.

Technically, various interactions between particles in PHPC and Fe/$C_{720}$ Buckyballs-Statin system are estimated by DREIDING and universal force field (UFF)[32,33]. The description of atomic systems and dynamics of biological molecules can be done by using these two effective force-fields[32,33]. Moreover, UFF contains interaction constants for every element of periodic table. By using general rules solely based upon the element, its hybridization, and its connectivity, the force-field parameters are chosen. In DREIDING and UFF force-fields, Lennard-Jones (LJ) formalism is applied for non-bond interactions between modeled particles[34]:

$$V(r_{ij}) = 4\varepsilon\left[\left(\frac{\sigma}{r_{ij}}\right)^{12} - \left(\frac{\sigma}{r_{ij}}\right)^{6}\right], r_{ij} \le r_c \quad (1)$$

where, $\varepsilon$ constant defines depth of the potential well, $\sigma$ constant represent distance which the interaction value is zero, and $r$ parameter is the distance between various particles inside MD box. Furthermore, $r_c$ constant introduced the cut off radius and accounts for 12 Å in our simulations. The $\varepsilon$ and $\sigma$ parameters for PHPC and Fe/$C_{720}$ Buckyballs-Statin system listed in **Table 1**.

**Table 1.** The length and energy parameters for LJ interaction inside computational box[32,33].

| **Element** | **$\varepsilon$ (kcal/mol)** | **$\sigma$ (Å)** |
|---|---|---|
| C | 0.105 | 3.851 |
| H | 0.044 | 2.886 |
| Cl | 0.227 | 3.947 |
| N | 0.069 | 3.660 |
| O | 0.060 | 3.500 |
| P | 0.305 | 4.147 |
| S | 0.274 | 4.035 |
| Fe | 0.013 | 2.912 |

On the other hand, in DREIDING and UFF force-fields harmonic formalism implemented for various bonding interactions[35]:

$$V(r) = k_r(r - r_0) \quad (2)$$

$$V(\theta) = k_\theta(\theta - \theta_0) \quad (3)$$

The $k_r/k_\theta$ represents harmonic constant and $r_0/\theta_0$ presents the equilibrium distance/angle of inter-atomic bonds. Next, Newton's law at the nano-scale has been used as the gradient of the defined force-fields for computations of the time evolution of defined[35]:

$$F_i = \sum_{i \neq j} F_{ij} = m_i \frac{d^2 r_i}{dt^2} = -\nabla V \quad (4)$$

in this equation, $F$ represents the total force, $r_i$ is the position, $m_i$ is the mass and $v_i$ is the velocity of particle $i$. The following equations represent the integration of the Newton law by the prevalent Velocity-Verlet approach, to associate the previous formulations[36–38]:

$$r(t + \Delta t) = r(t) + v(t)\Delta t + \frac{1}{2}a(t)\Delta t^2 + O(\Delta t^4) \quad (5)$$

$$v(t + \Delta t) = v(t) + \frac{a(t) + a(t + \Delta t)}{2} + O(\Delta t^2) \quad (6)$$

in these equations, $r$ and $v$ parameters defined position and velocity of particles in various time steps, respectively. Computationally, we can say our MD study done in the following two main steps via described simulation method:

Step A: Atomic interaction between PHPC and Fe/$C_{720}$ Buckyballs-Statin structures was simulated at the defined initial condition. The simulation box has 250 Å length in *X*, *Y*, and *Z* directions and periodic boundary condition defined for them[35]. Here, modeled samples temperature and pressure was equilibrated at 300 K and 1 bar as initial condition. Time step value for this process setting set to 1 fs. Technically, we used Nose-Hoover algorithm with 10 and 100 damping ratio for temperature and pressure parameters[39–42]. Described simulations done for $t$ = 10 ns and potential energy variation of PHPC and Fe/$C_{720}$ Buckyballs-Statin samples calculated for verifying of our computational settings.

Step B: Next, PHPC and Fe/$C_{720}$ Buckyballs-Statin system were simulated in the unit computational box. The atomic interaction between PHPC and Fe/$C_{720}$ Buckyballs-Statin atomic compound was carried out by using NVT ensemble for 10 ns. For analyzing the atomic evolution of modeled system, various quantities such as total energy, distance of structures, diffusion coefficient and volume of atomic compounds were reported. Our computational study details listed in **Table 2**.

**Table 2.** MD simulation details in current computational research.

| **Computational parameter** | **Value/setting** |
|---|---|
| Computational box length | 250 × 250 × 250 $Å^3$ |
| Boundary condition | Periodic |
| Initial temperature | 300 K |
| Initial pressure | 1 bar |
| Time step | 1 fs |
| Computational ensembles | NPT/NVT |
| Temperature damping ratio | 10 |
| Pressure damping ratio | 100 |
| Equilibrium time | 10 ns |
| Total simulation time | 30 ns |

## 3. Results of MD simulations and discussions

Firstly, the equilibrium phase of PHPC and Fe/$C_{720}$ Buckyballs-Statin system was studied and final arrangement of these compounds saved to next step of research as depicted in **Figure 2**. Snapshots of atomic compounds were visualized by OVITO visualization package[43]. Technically, Fe atoms added to pristine $C_{720}$ Buckyball (as atomic doping) to influence the magnetic field in the behavior of the atomic ball. MD outputs in current computational step indicated the initial arrangement of particles in PHPC and Fe/$C_{720}$ Buckyballs-Statin system is adopted with UFF and DREIDING potentials. Numerically, the thermodynamic stability of atomic system introduced by calculating of potential parameter inside MD box. **Figure 3** shows the potential energy of modeled samples as a function of MD simulation time. From this figure one can see, the potential parameter converged to finite value after 10 ns. The potential energy decreased by simulation time steps passing and converged to constant value. This atomic performance occurs in modeled samples by kinetic energy of particles increasing. By this evolution occur, the mean distance between various particles enlarged. Physically, potential energy has reciprocal relation with this distance. So, the potential and total energies of compounds converged to lesser values by enlarging this atomic parameter.

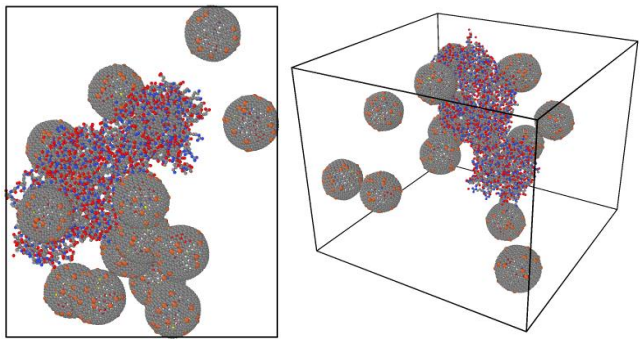

**Side view** **Perspective view**

**Figure 2.** Atomic representation of the PHPC and Fe/$C_{720}$ Buckyballs-Statin system simulated with LAMMPS package.

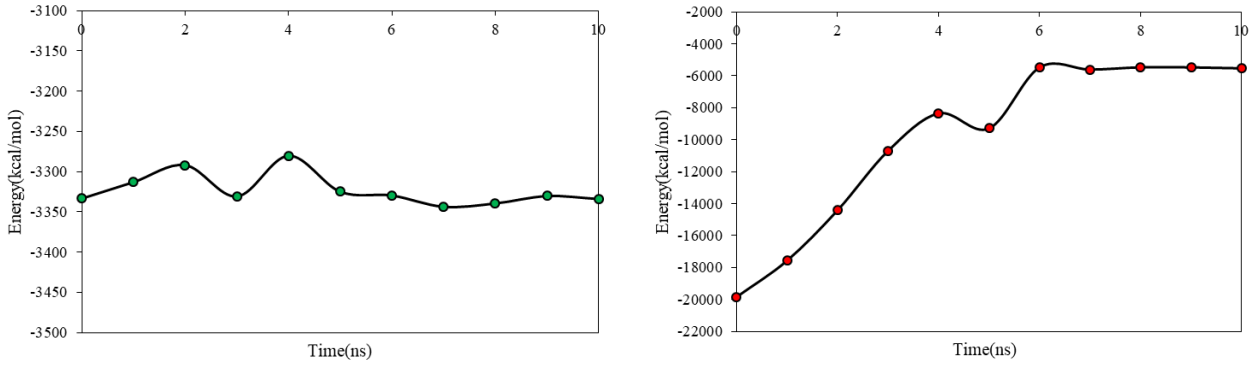


**(a)** **(b)**

**Figure 3.** Potential energy changes of **(a)** PHPC; **(b)** Fe/$C_{720}$ Buckyballs-Statin structures as a function of MD time.

After equilibrium phase detection in modeled sample, external field implemented to defined system. The formalism of plane, spherical and cylindrical external electric fields are as blow equations (respectively):

$$y = A\exp(ik.r - wt) \tag{7}$$

$$y = A\frac{\sin(k.r - wt)}{\sqrt{r}} \tag{8}$$

$$y = A\frac{\sin(k.r - wt)}{r} \tag{9}$$

MD outputs predicted 88 GHz value as normal frequency of defined compounds. Also, by setting frequency of plane, spherical and cylindrical external fields at 1.25, 1.71, and 1.73 GHz, the PHPC destruction process occur effectively (see **Figure 4**). Numerically, by implementing plane, spherical and cylindrical external fields, the destruction time of defined drug deliver compounds reached to 3.21, 3.05, and 3.82 ns (respectively) as listed in **Table 3**. Next, to study the interaction between PHPC and Fe/$C_{720}$ Buckyballs-Statin samples. These atomic structures interaction inside box done for 10 ns later. The equilibrated arrangement of each molecule exported from equilibration step and used in current computational section. The atomic evolution of defined compounds depicted in **Figures 4** and **5**. In this particle-base mixture, the initial distance of PHPC and Fe/$C_{720}$ Buckyballs-Statin lesser than $r_C$ parameter for simulation of particles interaction. The interaction energy variation of this system depicted in **Figure 6**. From this figure, the interaction energy of final structure bigger than each individual atomic structure's potential energy. Physically, the stability of defined samples has direct relation with this energy value. So interacting energy increasing verified the atomistic stability of final atomic mixture.

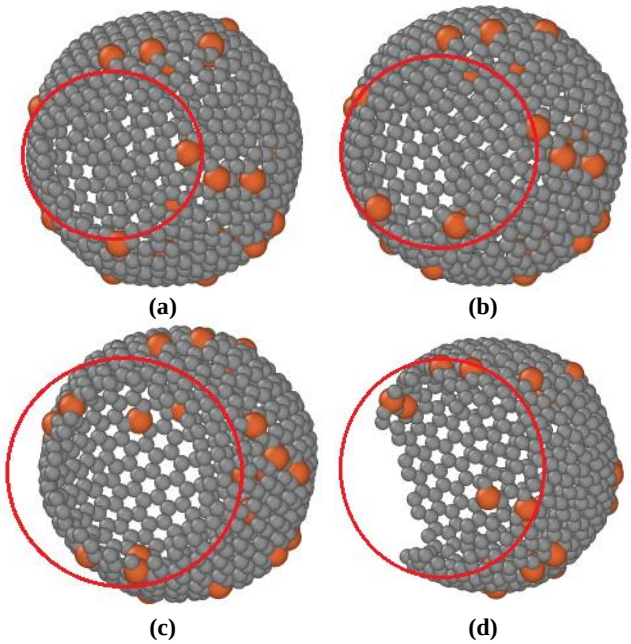


**Figure 4.** Atomic representation of simulated drug delivery system in presence of external field at **(a)** 3 ns; **(b)** 4 ns; **(c)** 5 ns; **(d)** 7 ns.

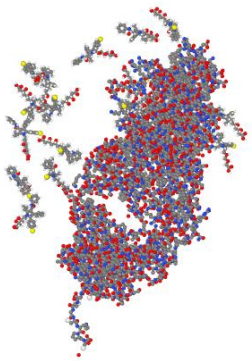

**Figure 5.** Atomic representation of defined PHPC and Fe/$C_{720}$ Buckyballs-Statin system after drug releasing process.

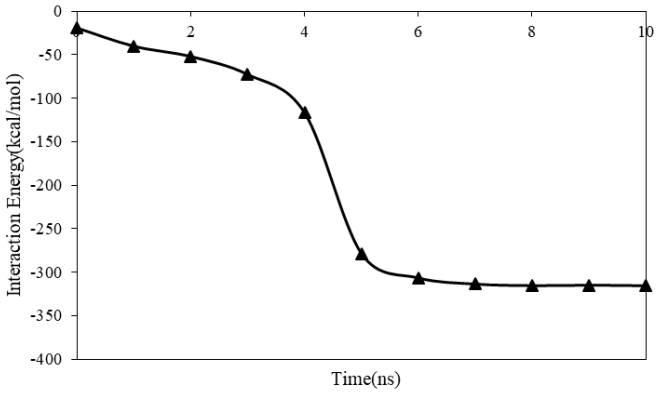


**Figure 6.** Interaction energy variation of PHPC and Fe/$C_{720}$ Buckyballs-Statin system by MD time passing.

**Table 3.** The destruction time of Fe/$C_{720}$ Buckyballs in presence of external field with various types.

| **External field type** | **Destruction time (ns)** |
|---|---|
| Plane | 3.21 |
| Spherical | 3.05 |
| Cylindrical | 3.82 |

After initial step of our computational research done and temperature/pressure equilibrium state of PHPC and Fe/$C_{720}$ Buckyballs-Statin system detected, canonical (NVT) ensemble continued for 10 ns. In thermodynamic, the accessible states of an atom-base system in thermal equilibrium with a heat bath at a finite initial temperature are defined by a NVT algorithm. In this computational procedure, the exchange of energy inside modeled system leads to a difference in the accessible energy states of final mixture. In this step, the center of mass (COM) variation of PHPC and drug-base sample has been reported by implementing NVT ensemble. From **Figure 7**, we concluded the net force type between various particles inside MD box is an attractive one. Numerically, the COM values of PHPC and Fe/$C_{720}$ Buckyballs-Statin samples varies from 10.27 Å to 2.96 Å (as reported in **Table 4**) at standard condition. This performance of modeled compounds arises from enlarging of the amplitude of particles movement. Physically, by atomic movement enlarging, the attraction ratio between modeled atoms decreases. So, we can conclude increasing the amplitude of atomic movement cause more particles penetration together. Atomic evolution of PHPC by drug diffusion to them depicted in **Figure 8**.

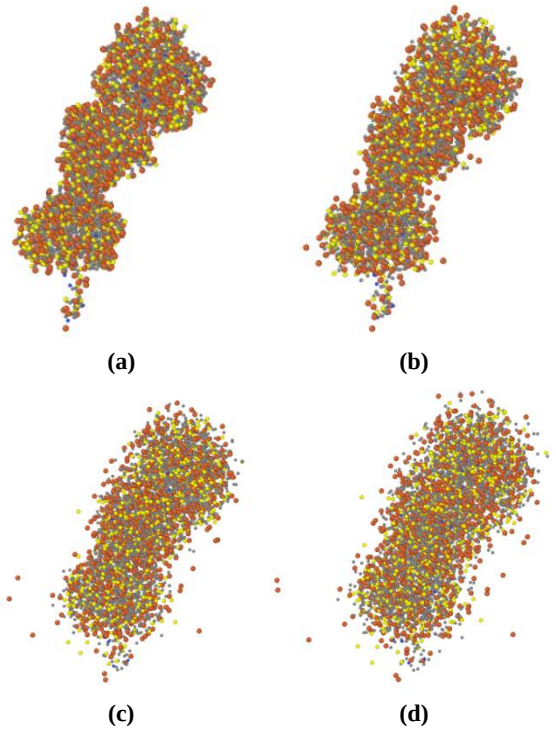


**Figure 7.** Atomic representation of human prostate protein at **(a)** 0 ns; **(b)** 1 ns; **(c)** 5 ns; **(d)** 10 ns.

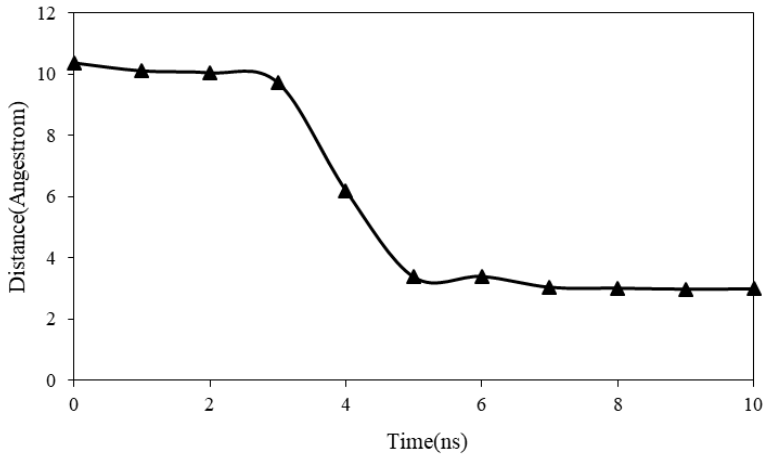


**Figure 8.** COM distance variation of PHPC and Fe/$C_{720}$ Buckyballs-Statin samples by time passing inside simulation box.

**Table 4.** COM distance of PHPC and Fe/$C_{720}$ Buckyballs-Statin samples as a function of MD time.

| MD time (ns) | COM distance (Å) |
|---|---|
| 0 | 10.27 |
| 1 | 10.01 |
| 2 | 9.95 |
| 5 | 3.34 |
| 10 | 2.96 |

The diffusion parameter is another numerical factor for describing various interactions (bonded/non-bonded) inside computational box. In this step of our computational research, to diffusion ratio estimation, MSD parameter of atomic compound has been calculated, by using the "compute/msd" command in LAMMPS input script. Computationally, the slope of this parameter versus time is proportional to the diffusion ratio (diffusion coefficient). Our results show that, by MD time enlarging the diffusion ratio increased to 1.153 $\mu m^2/s$. This atomistic parameter increasing arises from decreasing of total energy of PHPC-Buckyballs system which cause increasing the amplitude of particle's fluctuation. As the diffusion coefficient increases in MD simulations, the diffusion of PHPC into Fe/$C_{720}$ Buckyballs-Statin structure enlarged and the physical stability of protein-based sample decreases and this atomic structure is destructed by MD time steps passing. In bioinformatics, the root-mean-square deviation (RMSD), is the measure of the average distance between the atoms of superimposed proteins. Typically, RMSD is used as a quantitative measure atomic evolution of protein-based structures. Numerically, this parameter converged to 5.44 Å in PHPC sample after interaction occur between drug and protein as shown in **Figure 9** and **Table 5**. This process shows destruction process in PHPC sample inside MD box.

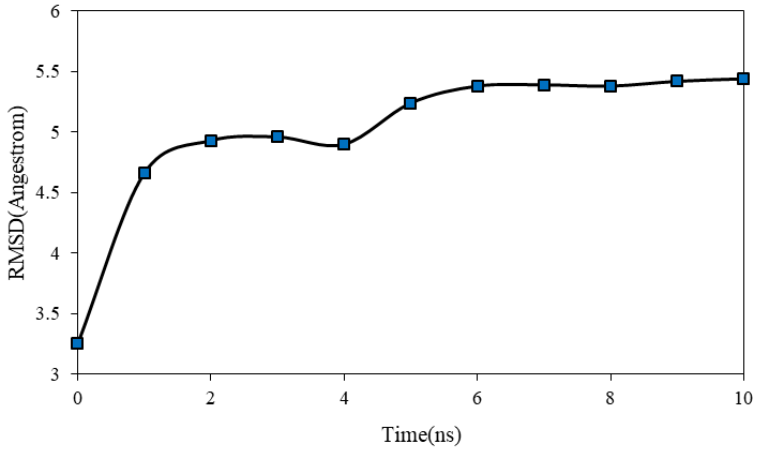


**Figure 9.** RMSD changes of PHPC sample by MD time steps passing.

**Table 5.** COM and RMSD parameters variation of modeled sample as a function of computational time.

| MD time (ns) | COM distance (Å) | RMSD (Å) |
|---|---|---|
| 0 | 10.27 | 3.25 |
| 1 | 10.01 | 4.66 |
| 2 | 9.95 | 4.93 |
| 5 | 3.34 | 5.24 |
| 10 | 2.96 | 5.44 |

The total volume of each atom-base samples is proportional to their physical stability. So, PHPC structure's volume changes indicated this compounds stability by MD time passing (from 0 to 10 ns). MD outputs indicated the volume of PHPC increases by more MD time steps passing. By enlarging the volume of

this compound, the atomic distance between protein particles increases. By this atomic evolution detection, total energy of protein decreases and stability of them converged to lesser ratio. Numerically, the volume of PHPC sample increases from 665,267 $Å^3$ to 737,143 $Å^3$ by MD time steps passing. Unlike the PHPC sample, $Fe/C_{720}$ Buckyballs-Statin's volume doesn't change appreciably by simulation time evolution as depicted in **Figure 10**. Our results show that, the volume of this atom-base compound varies from 25341 $Å^3$ to 26261 $Å^3$ by MD time passing (as listed in **Table 6**). Finally, we conclude that, the total energy decreasing in this step of computational research arises from PHPC's stability decreasing. **Figure 11** shows the volume changes of PHPC schematically. Technically, these figures and volume estimation have been done with "construct surface mesh" modifier of OVITO package.

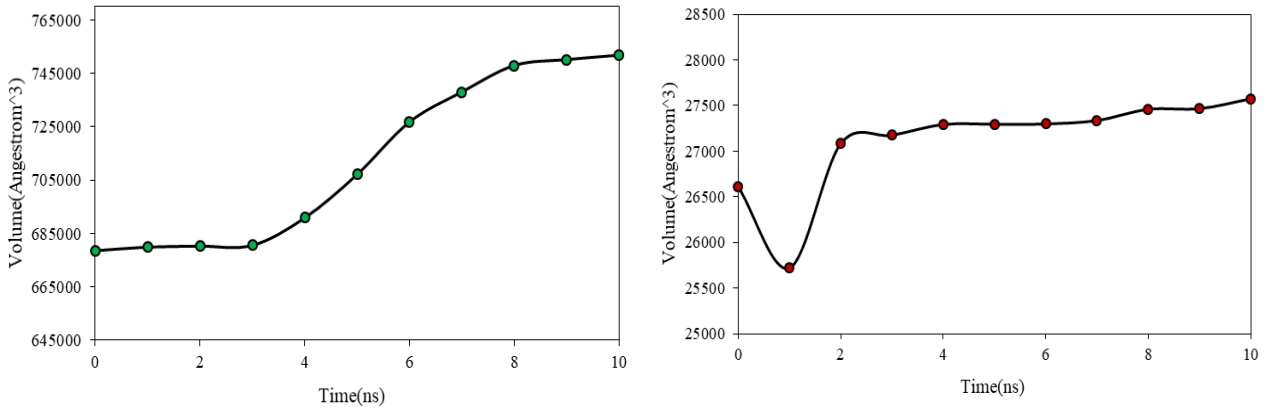


**(a)** **(b)**

**Figure 10.** Evolution of **(a)** PHPC; **(b)** $Fe/C_{720}$ Buckyballs-Statin structure's volume by MD time steps passing.

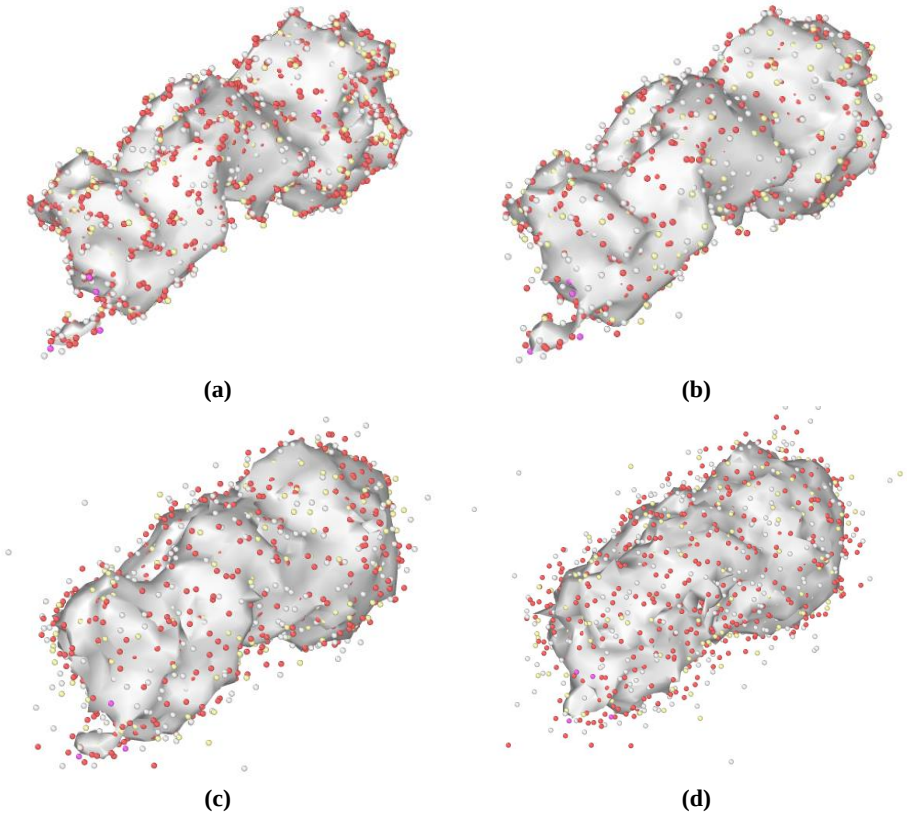

**(a)** **(b)**

**(c)** **(d)**

**Figure 11.** Evolution of PHPC structure's volume at **(a)** 0 ns; **(b)** 1 ns; **(c)** 5 ns; **(d)** 10 ns.

**Table 6.** PHPC (protein) and Fe/$C_{720}$ Buckyballs-Statin (drug) structure's volume changes as a function of MD time.

| MD time (ns) | Protein volume (Å$^3$) | Drug volume (Å$^3$) |
|---|---|---|
| 0 | 665,267 | 25,341 |
| 1 | 666,591 | 25,448 |
| 2 | 666,931 | 25,793 |
| 5 | 693,281 | 25,996 |
| 10 | 737,143 | 26,261 |

## 4. Conclusion

In current computational research, we study the effect of Fe/$C_{720}$ Buckyballs-Statin structure on atomic performance (destruction) of mediator protein of human prostate cancer (PHPC) via molecular dynamics (MD) approach. In this method, each PHPC and Fe/$C_{720}$ Buckyballs-Statin compounds is represented with atom by atom arrangement. Also, to simulate of interatomic force between various particles inside MD box, universal force field (UFF) and DREIDING force-field have been used inside simulation box. Our main outputs from MD simulations are as following:

- DREIDING and UFF atomic functions are appropriate for MD description of PHPC and Fe/$C_{720}$ Buckyballs-Statin samples. Numerically, the potential energy of modeled samples reached to ... kcal/mol after 10 ns. This physical performance shows the stability of this atom-base system.
- PHPC and Fe/$C_{720}$ Buckyballs-Statin sample's center of mass decreases from 10.27 Å to 2.96 Å by MD time steps passing.
- By increasing the diffusion of Fe/$C_{720}$ Buckyballs-Statin into PHPC sample, the stability of target protein converged to lesser ratios.
- The total volume of the PHPC enlarged by Fe/$C_{720}$ Buckyballs-Statin diffusion into this protein. Numerically, PHPC's volume 10.80% increase after atomic interaction with Fe/$C_{720}$ Buckyballs-Statin. By increasing this physical quantity, the stability of PHPC compound converged to lesser ratio.

Finally, we concluded Fe/$C_{720}$ Buckyball system can be used as drug-delivery system for Statin compound in PHPC destruction process for treatment of prostate cancer (in clinical cases).

## Author contributions

Conceptualization, MPP and RS; methodology, RS; software, MPP; validation, RS; formal analysis, RS; investigation, RS; resources, RS; data curation, RS; writing—original draft preparation, MPP; writing—review and editing, RS; visualization, MPP and RS; supervision, RS; project administration, RS; funding acquisition, RS. All authors have read and agreed to the published version of the manuscript.

## Acknowledgments

Support from the LAMMPS Tube computational center is gratefully acknowledged.

## Conflict of interest

The authors declare no conflict of interest.

## Nomenclature

| | |
|---|---|
| $F_{ij}$ | Force between various particles; |
| $m_i$ | Atomic mass; |

| | |
|---|---|
| $r_c$ | Cutoff parameter in LJ formalism; |
| $r_{ij}$ | Distance between various particles; |
| $t$ | MD time step; |
| $v_i$ | Atomic velocity; |
| $k_\theta$ | Constant parameter in angular harmonic formalism; |
| $k_r$ | Constant parameter in simple harmonic formalism; |
| $r_0$ | Equilibrium distance in simple harmonic formalism; |
| $V$ | atomic potential function. |

Greek symbols:

| | |
|---|---|
| $\varepsilon$ | Atomic energy in LJ formalism; |
| $\sigma$ | Distance constant in LJ formalism; |
| $\phi$ | Potential function of atomic systems; |
| $\theta_0$ | Equilibrium angle in angular harmonic formalism. |

# References


1. Bray F, Ferlay J, Soerjomataram I, et al. Global cancer statistics 2018: GLOBOCAN estimates of incidence and mortality worldwide for 36 cancers in 185 countries. CA: A Cancer Journal for Clinicians. 2018; 68(6): 394-424. doi: 10.3322/caac.21492
2. Koh KA, Sesso HD, Paffenbarger RS, et al. Dairy products, calcium and prostate cancer risk. British Journal of Cancer. 2006; 95(11): 1582-1585. doi: 10.1038/sj.bjc.6603475
3. Caini S, Gandini S, Dudas M, et al. Sexually transmitted infections and prostate cancer risk: A systematic review and meta-analysis. Cancer Epidemiology. 2014; 38(4): 329-338. doi: 10.1016/j.canep.2014.06.002
4. Lee MV, Katabathina VS, Bowerson ML, et al. BRCA-associated Cancers: Role of Imaging in Screening, Diagnosis, and Management. RadioGraphics. 2017; 37(4): 1005-1023. doi: 10.1148/rg.2017160144
5. Catalona WJ. Prostate Cancer Screening. Medical Clinics of North America. 2018; 102(2): 199-214. doi: 10.1016/j.mcna.2017.11.001
6. Grossman DC, Curry SJ, Owens DK, et al. Screening for Prostate Cancer. JAMA. 2018; 319(18): 1901. doi: 10.1001/jama.2018.3710
7. Cabarkapa S, Perera M, McGrath S, et al. Prostate cancer screening with prostate-specific antigen: A guide to the guidelines. Prostate International. 2016; 4(4): 125-129. doi: 10.1016/j.prnil.2016.09.002
8. Stratton J, Godwin M. The effect of supplemental vitamins and minerals on the development of prostate cancer: a systematic review and meta-analysis. Family Practice. 2011; 28(3): 243-252. doi: 10.1093/fampra/cmq115
9. Luszczak S, Kumar C, Sathyadevan VK, et al. PIM kinase inhibition: co-targeted therapeutic approaches in prostate cancer. Signal Transduction and Targeted Therapy. 2020; 5(1). doi: 10.1038/s41392-020-0109-y
10. World Health Organization. Chapter 1.1. World Cancer Report. World Health Organization; 2014.
11. Baade PD, Youlden DR, Krnjacki LJ. International epidemiology of prostate cancer: Geographical distribution and secular trends. Molecular Nutrition & Food Research. 2009; 53(2): 171-184. doi: 10.1002/mnfr.200700511
12. Leslie SW, Soon-Sutton TL, Sajjad H, Siref LE. Prostate Cancer. In: StatPearls. Treasure Island (FL): StatPearls Publishing; 2020.
13. Miller DC, Hafez KS, Stewart A, et al. Prostate carcinoma presentation, diagnosis, and staging. Cancer. 2003; 98(6): 1169-1178. doi: 10.1002/cncr.11635
14. Van der Cruijsen-Koeter IW, Vis AN, Roobol MJ, et al. Comparison of screen detected and clinically diagnosed prostate cancer in the European randomized study of screening for prostate cancer, section rotterdam. Journal of Urology. 2005; 174(1): 121-125. doi: 10.1097/01.ju.0000162061.40533.0f
15. Calle EE, Rodriguez C, Walker-Thurmond K, et al. Overweight, Obesity, and Mortality from Cancer in a Prospectively Studied Cohort of U.S. Adults. New England Journal of Medicine. 2003; 348(17): 1625-1638. doi: 10.1056/nejmoa021423
16. Menez R, Stura E, Jolivet-Reynaud C. Crystal structure of human prostate specific antigen complexed with an activating antibody. J Mol Biol. 2008; 376: 1021-1033. doi: 10.2210/pdb2ZCH/pdb
17. Winsberg E. Science in the Age of Computer Simulation. Chicago: University of Chicago Press; 2010.
18. Humphreys P. Extending Ourselves: Computational Science, Empiricism, and Scientific Method. Oxford: Oxford University Press; 2004
19. Nutaro JJ. Building Software for Simulation: Theory and Algorithms, with Applications in C++. John Wiley & Sons; 2011.
20. Schlick T. Pursuing Laplace's Vision on Modern Computers. Mathematical Approaches to Biomolecular Structure and Dynamics. The IMA Volumes in Mathematics and its Applications. 1996; 82: 219-247. doi: 10.1007/978-1-

4612-4066-2_13
21. Alder BJ, Wainwright TE. Studies in Molecular Dynamics. I. General Method. The Journal of Chemical Physics. 1959; 31(2): 459-466. doi: 10.1063/1.1730376
22. Rahman A. Correlations in the Motion of Atoms in Liquid Argon. Physical Review. 1964; 136(2A): A405-A411. doi: 10.1103/physrev.136.a405
23. Jolfaei NA, Jolfaei NA, Hekmatifar M, et al. Investigation of thermal properties of DNA structure with precise atomic arrangement via equilibrium and non-equilibrium molecular dynamics approaches. Computer Methods and Programs in Biomedicine. 2020; 185: 105169. doi: 10.1016/j.cmpb.2019.105169
24. Ashkezari AZ, Jolfaei NA, Jolfaei NA, et al. Calculation of the thermal conductivity of human serum albumin (HSA) with equilibrium/non-equilibrium molecular dynamics approaches. Computer Methods and Programs in Biomedicine. 2020; 188: 105256. doi: 10.1016/j.cmpb.2019.105256
25. Koehl P, Levitt M. A brighter future for protein structure prediction. Nature Structural Biology. 1999; 6(2): 108-111. doi: 10.1038/5794
26. Sabetvand R, Ghazi ME, Izadifard M. Studying temperature effects on electronic and optical properties of cubic CH3NH3SnI3 perovskite. Journal of Computational Electronics. 2020; 19(1): 70-79. doi: 10.1007/s10825-020-01443-3
27. Wang LP, Martinez TJ, Pande VS. Building Force Fields: An Automatic, Systematic, and Reproducible Approach. The Journal of Physical Chemistry Letters. 2014; 5(11): 1885-1891. doi: 10.1021/jz500737m
28. Plimpton S. Fast Parallel Algorithms for Short-Range Molecular Dynamics. Journal of Computational Physics. 1995; 117(1): 1-19. doi: 10.1006/jcph.1995.1039
29. Plimpton SJ, Thompson AP. Computational aspects of many-body potentials. MRS Bulletin. 2012; 37(5): 513-521. doi: 10.1557/mrs.2012.96
30. Brown WM, Wang P, Plimpton SJ, et al. Implementing molecular dynamics on hybrid high performance computers – short range forces. Computer Physics Communications. 2011; 182(4): 898-911. doi: 10.1016/j.cpc.2010.12.021
31. Brown WM, Kohlmeyer A, Plimpton SJ, et al. Implementing molecular dynamics on hybrid high performance computers – Particle–particle particle-mesh. Computer Physics Communications. 2012; 183(3): 449-459. doi: 10.1016/j.cpc.2011.10.012
32. Rappe AK, Casewit CJ, Colwell KS, et al. UFF, a full periodic table force field for molecular mechanics and molecular dynamics simulations. Journal of the American Chemical Society. 1992; 114(25): 10024-10035. doi: 10.1021/ja00051a040
33. Mayo SL, Olafson BD, Goddard WA. DREIDING: a generic force field for molecular simulations. The Journal of Physical Chemistry. 1990; 94(26): 8897-8909. doi: 10.1021/j100389a010
34. Lennard-Jones JE. On the Determination of Molecular Fields. Proc. R. Soc. Lond. A. 1924; 106(738): 463-477. doi: 10.1098/rspa.1924.0082
35. Rapaport DC, Blumberg RL, McKay SR, et al. The Art of Molecular Dynamics Simulation. Computers in Physics. 1996; 10(5): 456-456. doi: 10.1063/1.4822471
36. Verlet L. Computer "Experiments" on Classical Fluids. I. Thermodynamical Properties of Lennard-Jones Molecules. Physical Review. 1967; 159(1): 98-103. doi: 10.1103/physrev.159.98
37. Press WH, Teukolsky SA, Vetterling WT, Flannery BP. Section 17.4. Second-Order Conservative Equations. In: Numerical Recipes: The Art of Scientific Computing, 3rd ed. New York: Cambridge University Press; 2007.
38. Hairer E, Lubich C, Wanner G. Geometric numerical integration illustrated by the Störmer-Verlet method. Acta Numerica. 2003; 12: 399–450. doi: 10.1017/S0962492902000144
39. Nosé S. A unified formulation of the constant temperature molecular dynamics methods. The Journal of Chemical Physics. 1984; 81(1): 511-519. doi: 10.1063/1.447334
40. Hoover WG. Canonical dynamics: Equilibrium phase-space distributions. Physical Review A. 1985; 31(3): 1695-1697. doi: 10.1103/physreva.31.1695
41. Hoover WG, Holian BL. Kinetic moments method for the canonical ensemble distribution. Physics Letters A. 1996; 211(5): 253-257. doi: 10.1016/0375-9601(95)00973-6
42. Welty JR, Wicks CE, Wilson RE, Rorrer G. Fundamentals of Momentum, Heat, and Mass Transfer. Wiley; 2001.
43. Stukowski A. Visualization and analysis of atomistic simulation data with OVITO–the Open Visualization Tool. Modelling and Simulation in Materials Science and Engineering. 2009; 18(1): 015012. doi: 10.1088/0965-0393/18/1/015012